Cambridge Centre for Computational Chemical Engineering

University of Cambridge

Department of Chemical Engineering

Preprint ISSN 1473 – 4273

Modelling Nanoparticle Dynamics: Coagulation, Sintering, Particle Inception and Surface Growth

Neal Morgan[1], Clive Wells[1], Markus Kraft[1],

Wolfgang Wagner[2]

submitted: December 9, 2003

[1] Department of Chemical Engineering
University of Cambridge
Pembroke Street
Cambridge CB2 3RA
UK
e-Mail: nmm22@cam.ac.uk,
cgw11@cam.ac.uk,
markus_kraft@cheng.cam.ac.uk

[2] Weierstrass Institute
for Applied Analysis and Stochastics
Mohrenstrasse 39
10117 Berlin
Germany
e-Mail: wagner@wias-berlin.de

Preprint No. 19

c4e

Key words and phrases. Nanoparticles, Particle Size Distribution, Stochastic Processes.

Edited by
Cambridge Centre for Computational Chemical Engineering
Department of Chemical Engineering
University of Cambridge
Cambridge CB2 3RA
United Kingdom.

Fax: + 44 (0)1223 334796
E-Mail: c4e@cheng.cam.ac.uk
World Wide Web: http://www.cheng.cam.ac.uk/c4e/

Abstract

In this paper we investigate a new stochastic particle method (SPM) for solving an extension to the sintering-coagulation equation and model two particle systems: the production of SiO_2 and TiO_2. A model which includes both a particle source and an area dependent surface growth term as well as coagulation and sintering is presented. A new mass-flow stochastic algorithm to solve the model is stated. The stochastic method is able to recover fully the evolution the bivariate particle size distribution function (PSDF) and is computationally very efficient when compared to traditional finite element methods. The SPM is compared to a bivariate sectional method for a system with coagulation and sintering as the only mechanisms. Despite using a different form of coagulation kernel to the sectional investigation, the results obtained agree closely to those in the literature and were obtained in a small fraction of the time. The full model with particle inception and surface growth was then used to model the $TiCl_4 \rightarrow TiO_2$ system under various conditions. At low precursor concentration we investigate the effect of changing temperature, whilst at high precursor concentration we investigate the effect of surface growth on the system. The results agree with many of the conclusions reached in the literature.

Contents

1 Introduction

The ability to model the particle size distribution (PSD) of a nanoparticle system is extremely important as the size and shape of the particles may affect the physical attributes of the final product. The use of population balance models to study nanoparticle growth has become widespread, especially when studying nanoparticles formed in flames [5, 11, 12, 10]. Mechanisms that focus on more than one variable (e.g., particle mass and surface area) can be simulated and represent a more complete picture of what is happening in the system.

Bivariate population balances have been solved in the past using sectional (finite element) methods. These methods show the evolution of the PSD however, the reported computational times associated with this method (of the order of days) make it an impractical method to use. Stochastic particle methods (SPMs) are also able to model the PSD evolution but without the added computational cost.

Stochastic methods have been used previously to study univariate nanoparticle dynamics with a source term [2, 3] and bivariate dynamics that include coagulation and sintering [13, 15]. The purpose of this paper is to extend the model to include surface growth as well as particle inception, coagulation and sintering, and introduce a new mass-flow stochastic algorithm. The mass-flow algorithm has a major advantage over the direct-simulation algorithm: the variance of important functionals is reduced compared to a similar direct simulation algorithm.

The stochastic particle approach represents the system as an ensemble of N stochastic particles. These particles interact according to the relative rates of the various processes involved in the simulation. We make no assumptions about the final shape of the PSD. The number of stochastic particles used in the simulation determines the accuracy of the simulation. It has be shown for a simple univariate system undergoing coagulation and fragmentation [1] that as $N \to \infty$ the particle system converges to the solution of the model. The convergence properties of the pure coagulation-sintering algorithm have been investigated in [15] and the error was found to be of the order $N^{-1/2}$ whilst the complexity of the algorithm is of the order $N\log N$.

For the first time, the method outlined above is applied to two systems. The first system is that used in [7] for particles of SiO_2 at various temperatures, simulating the coagulation and sintering behaviour. The second system is that of $TiCl_4$ oxidation to TiO_2 and includes the full model for particle inception and surface growth together with coagulation and sintering.

2 The Particle Model

The equation used to describe the evolution of the particle sizes with time is the coagulation-sintering equation [16] which is an extension to the Smoluchowski coagulation equation [14]. We add two further terms to the equation to model a particle

source and surface growth of the particles:

$$\frac{\partial}{\partial t}n_t(v,a) = \frac{\partial}{\partial a}\left(\frac{1}{t_0}\left[a - a_0\left(\frac{v}{v_0}\right)^{2/3}\right]n_t(v,a)\right)$$
$$+\frac{1}{2}\int_{v_0}^{v}\int_{a_0\left(\frac{v'}{v_0}\right)^{2/3}}^{\frac{a_0 v'}{v_0}}\beta_{v',v-v'}(a',a-a')n_t(v',a')n_t(v-v',a-a')\mathrm{d}a'\mathrm{d}v'$$
$$-n_t(v,a)\int_{v_0}^{\infty}\int_{a_0\left(\frac{v'}{v_0}\right)^{2/3}}^{\frac{a_0 v'}{v_0}}\beta_{v,v'}(a,a')n_t(v',a')\mathrm{d}a'\mathrm{d}v'$$
$$+k_{\mathrm{g}}Cn^{in} + k_{\mathrm{s}}C\left[(a-a_0)n_t(v-v_0,a-a_0) - an_t(v,a)\right] \qquad (2.1)$$

with the initial condition $n_0(v,a)$, where v and a are volume and surface area respectively. The gas phase concentration (C) is determined by the following equation,

$$\frac{\mathrm{d}C}{\mathrm{d}t} = -k_{\mathrm{tot}}C, \qquad (2.2)$$

where k_{tot} is the total rate of loss of the gas phase precursor.

The model can be split into four distinct parts that represent the four processes that are being simulated: sintering, coagulation, particle inception and surface growth. The first part of the right hand side of Eqn. 2.1 describes the sintering of particles. The expression in the square brackets determines the difference between the current area of a particle and its spherical minimum. The parameter t_0 is the characteristic sintering time and takes the form of a function of temperature (T) and particle diameter (d_p). If the sintering is determined by viscous flow then the sintering time is proportional to d_p and is of the form

$$t_0 = \frac{\mu d_p}{\sigma}, \qquad (2.3)$$

where μ is the viscosity and σ is the surface energy of the particulate matter. If the sintering is determined by boundary diffusion then the sintering time is of the form

$$t_0 = A_{\mathrm{sint}}Td_p^4\ \exp\left(\frac{B_{\mathrm{sint}}}{T}\right), \qquad (2.4)$$

where A_{sint} and B_{sint} are constants depending on the system being simulated. In general we will take the characteristic sintering time to take the form

$$t_0 = t_1 f(v/v_0, a/a_0, T/T_0) = t_1 f(\nu,\sigma,\theta), \qquad (2.5)$$

where v_0 and a_0 are the volume and surface area of the primary particles and T_0 is the initial temperature.

The second and third lines of Eqn. 2.1 describe the coagulation of particles within the system. The first is a birth term and the second is a death term.

The coagulation kernel, $\beta_{v,v'}(a,a')$ can be written as

$$\beta_{v,v'}(a,a') = \left(\frac{k_b T_0 a_0^2}{2\pi m_0}\right)^{\frac{1}{2}}\theta^{\frac{1}{2}}K(x,x'), \qquad (2.6)$$

where k_b is Boltzmann's constant, m_0 is the mass of a primary particle and $K(x, x')$ is a dimensionless form where $x = (\nu, \sigma)$. The kernel, $K(x, x')$ is given by:

$$K(x, x') = \left(\frac{1}{\nu} + \frac{1}{\nu'}\right)^{\frac{1}{2}} \left[(s(\nu)\sigma)^{\frac{1}{2}} + (s(\nu')\sigma')^{\frac{1}{2}}\right]^2. \tag{2.7}$$

The function $s(\nu)$ is the surface area accessability function and is given by

$$\begin{aligned} s(\nu) &= \lambda_1 \nu^{\alpha-1} + \lambda_2; \\ \lambda_1 &= 2^{1-\alpha}(D_S - 2); \\ \lambda_2 &= 3 - D_S, \end{aligned} \tag{2.8}$$

where $D_S \in [2, 3]$ is a surface fractal dimension and $\alpha \in [0, 1]$ is the surface area scaling factor.

The first term on the fourth line of Eqn. 2.1 describes particles entering the system from the gas phase. The parameter k_{g} is the gas-phase oxidation rate.

The final term of Eqn. 2.1 describes the deposition of new mass onto the surface of a particle. As with the particle coagulation term, the surface growth term has a birth-death part. The quantity $k_{\mathrm{s}}A_s$ is the surface oxidation rate where A_s is the surface area density of the system.

The overall rate for the production of new mass in the system is equal to the the sum of the gas-phase (k_{g}) and surface growth ($k_{\mathrm{s}}A_s$) rates:

$$k_{\mathrm{tot}} = k_{\mathrm{g}} + k_{\mathrm{s}}A_s. \tag{2.9}$$

The particle size distribution function (PSDF), $n_t(v, a)$ is multiplied by a constant term to obtain a dimensionless PSDF, $N_\tau(x)$ thus:

$$N_\tau(x) = v_0 a_0^2 t_1 \left(\frac{k_b T_0}{2\pi m_0}\right)^{\frac{1}{2}} n_t(v, a) = \xi n_t(v, a), \tag{2.10}$$

where τ is a dimensionless time, given by $\tau = t/t_1$. This allows Eqn. 2.1 to be converted to a dimensionless form:

$$\begin{aligned} \frac{\partial}{\partial \tau} N_\tau(x) = \frac{\partial}{\partial \sigma}\left(\frac{1}{f(\sigma, \nu, \theta)}\left[\sigma - \nu^{2/3}\right] N_\tau(x)\right) \\ + \frac{1}{2}\int_1^{\nu}\int_{\nu'^{2/3}}^{\nu'} \theta^{1/2} K(x, x - x') N_\tau(x') N_\tau(x - x') \mathrm{d}\sigma' \mathrm{d}\nu' \\ - N_\tau(x)\int_1^{\infty}\int_{\nu'^{2/3}}^{\nu'} \theta^{1/2} K(x, x') N_\tau(x') \mathrm{d}\sigma' \mathrm{d}\nu' \\ + \frac{k_g C \xi t_1}{v_0 a_0}\delta(\sigma - 1)\delta(\nu - 1) \\ + a_0 t_1 k_s C\left[(\sigma - 1) N_\tau(x - 1) - \sigma N_\tau(x)\right], \end{aligned} \tag{2.11}$$

where we define $(x - 1) = (\nu - 1, \sigma - 1)$.

3 The Stochastic Particle Algorithm

Casting Eqn. 2.11 into a weak mass flow form allows us to write down the stochastic generators of the various processes that the model describes and hence determine their contributions to the stochastic simulation [15, 6]. To make the simulation more efficient, we use the majorant kernel, $\hat{K}(x, x')$ introduced in [15]. This reduces the complexity of the algorithm compared to using $K(x, x')$ explicitly. The majorant kernel takes the form:

$$\hat{K}(x, x') = 2\left(\omega(x) + \psi(x)\nu'^{-\frac{1}{2}} + \psi(x')\nu^{-\frac{1}{2}} + \omega(x')\right), \tag{3.1}$$

where

$$\begin{aligned} \omega(x) &= \lambda_1\sigma\nu^{\alpha-3/2} + \lambda_2\sigma\nu^{\frac{1}{2}} \quad \text{and} \\ \psi(x) &= \lambda_1\sigma\nu^{\alpha-1} + \lambda_2\sigma. \end{aligned} \tag{3.2}$$

Sintering is dealt with by introducing a finite step size parameter, Λ. This parameter determines the discretization of surface area and hence the sintering time step parameter, ϱ_Λ given by

$$\varrho_\Lambda(x) = \begin{cases} \frac{\Lambda^{-1}\left(\sigma-\nu^{\frac{2}{3}}\right)}{f(\nu,\sigma,\theta)} & \text{if } \nu^{\frac{2}{3}} + \Lambda \leq \sigma \leq \nu, \\ 0 & \text{otherwise.} \end{cases} \tag{3.3}$$

It is important to note that the algorithm used in this paper is a mass flow algorithm. Mass-flow coagulation is a constant N operation and so to conserve this property for other operators, we introduce an overall scaling factor for the simulation that changes as new mass enters the system. The scaling of the simulation (κ) is determined by

$$\kappa = \frac{n_0(v, a)\xi}{N}, \tag{3.4}$$

Each time a new particle enters the system, κ is increased by a factor of $N/(N-1)$.

A second point of note is that in the mass-flow algorithm, surface growth is implemented as two separate jumps, each with its own rate. For a further explanation, see [6].

The simulation proceeds as follows:

1. Generate initial state, p, and calculate κ.
2. Calculate the total surface area density of the system, A_s from:

$$A_s = \frac{a_0^2 v_0 \kappa}{\xi} \sum_{i=1}^{N} \frac{\sigma_i}{\nu_i},$$

   calculate k_{tot} from:

$$k_{\text{tot}} = k_{\text{g}} + k_{\text{s}} A_s,$$

   and hence numerically integrate Eqn. 2.2 to calculate the new concentration of the gas phase precursor, C.

3. Wait an exponentially distributed time step τ, with parameter $\hat{\rho}(p)$ equal to the sum of the rates of the processes:

$$\hat{\rho}(p) = \rho_{\text{sint}}(p) + \hat{\rho}_{\text{coag}}(p) + \rho_{\text{inf}}(p) + \rho_{\text{Surf}_1}(p) + \rho_{\text{Surf}_2}(p)$$

$$\hat{\rho}(p) = \sum_{i=1}^{N} \varrho_{\Lambda}(x_i) + \kappa\theta^{1/2} \sum_{i,j=1}^{N} \frac{\hat{K}(x_i, x_j)}{\nu_j} + \frac{k_g C \xi t_1}{v_0 a_0 \kappa} + a_0 t_1 k_{\text{s}} C \sum_{i=1}^{N} \sigma_i + a_0 t_1 k_{\text{s}} C \left(\frac{N-1}{N}\right) \sum_{i=1}^{N} \frac{\sigma_i}{\nu_i},$$

and increase time according to

$$t \mapsto t + \tau$$

if $t \geqslant t_{stop}$ then stop simulation, else go to 4.

4. Choose one of the events probabilistically according to their relative rates.
For sintering, go to 5
for particle inception, go to 6
for surface growth (type one) go to 7
for surface growth (type two) go to 8
for coagulation go to 9.

5. Perform a sintering step:
   (a) choose a particle i according to the distribution $\varrho_{\Lambda}(x_i)$ and reduce the surface area of the particle by an amount Λ.
   (b) go to 2.

6. Perform a particle inception step:
   (a) Add a cluster of size 1 to the system and remove one of size x where x is chosen uniformly from the particle array.
   (b) go to 2.

7. Perform a surface growth step (type 1):
   (a) Choose a particle, i, according to the distribution:

$$\frac{\sigma_i}{\sum_{k=1}^{N} \sigma_i}$$

   (b) Remove particle i and replace with a particle of size $(\nu_i + 1, \sigma_i + 1)$
   (c) go to 2.

8. Perform a surface growth step (type 2):

(a) Choose a particle, i, according to the distribution:

$$\frac{\sigma_i/\nu_i}{\sum_{k=1}^{N}\sigma_i/\nu_i}$$

and a particle j uniformly.

(b) Remove particle j and replace with a particle of size $(\nu_i + 1, \sigma_i + 1)$

(c) go to 2.

9. Perform a coagulation step:

(a) Choose particles i and j according to the distribution:

$$\frac{\frac{\hat{K}(x_i,x_j)}{\nu_j}}{\sum_{i,j}\frac{\hat{K}(x_j,x_j)}{\nu_j}}, \qquad i \neq j$$

(b) With probability

$$\frac{K(x_i, x_j)}{\hat{K}(x_i, x_j)}$$

add a particle of size $(x_i + x_j)$ to the particle ensemble and remove one of size x_i. Otherwise the jump is fictitious and the particles have not interacted.

(c) go to 2.

4 Results

4.1 Silica undergoing sintering and coagulation

The algorithm's performance was compared to that of a bivariate sectional method by simulating the system described in [7].

The characteristic sintering time associated with this simulation is of the form of Eqn. 2.4, with the sintering time constants, A_{sint} and B_{sint} coming from [4]. The parameters used in the simulations are set out in Table 1.

Table 1: *Parameters for* SiO_2 *simulation.*

Parameter	Value
C_0	$10^{22}\,\text{m}^{-3}$
t_{stop}	$10^{-4}\,\text{s}$
T	$573/773/1073\,\text{K}$
A_{sint}	$1.838 \times 10^{10}\,\text{K}^{-1}\text{m}^{-4}\text{s}$
B_{sint}	$2.766 \times 10^{4}\,\text{K}$
N	8192

In Fig. 1 various properties for the stochastic particle system are plotted. The average particle diameter (Fig. 1(b)) is calculated using

$$d_p = \frac{6v}{a}. \tag{4.1}$$

With this in mind, we see that sintered particles will have a larger calculated value of d_p. If we compare the results calculated by the stochastic method to the ones obtained is [7] we see that in general the correlation is good. We believe the discrepancies arise due to that fact that a different form of coagulation kernel was used in the sectional investigation. At high temperatures, the two kernels behave very similarly and hence the results are in good agreement. It is worth noting that the run time for the simulation at 1073K with 8192 particles took just over 240 seconds to run on an Athlon 1.2GHz PC. This compares very well with the run time mentioned in [7] of 112 days however since no estimate of error is made in the paper, an exact comparison is not possible.

Figure 2 shows the extent to which the particles have sintered, given the temperature for which the system was simulated. At higher temperatures, the characteristic sintering time of particles is considerably less than at lower temperatures. For example, the sintering time of a medium sized particle changes by 14 orders of magnitude when we change the temperature from 500K to 1200K. The figure shows that at 573K no sintering occurs and we only get aggregates. At 773K some sintering occurs and the particles deviate from the line of pure coagulation. Finally at 1073K we get complete sintering and all particles lie on the line of total sintering.

4.2 Titania Reaction Simulation

The $TiCl_4$ gas phase kinetics are described by a very simple reaction scheme that incorporates both the gas-phase oxidation and surface oxidation processes. The rates for the surface oxidation and gas-phase oxidation were taken to be the same as those used in [11], k_g and k_s taking the form of a simple Arrhenius equation ($k = A\exp(-E_A/RT)$). The simulations were run using the conditions in Table 2 ('gas' refers to the gas phase oxidation rate and 'surf' the surface oxidation rate). Sintering was taken to be boundary diffusion with A_sint and B_sint taken from [16].

Figure 3 shows the evolution of the marginal PSDs. In Fig. 3(a) and Fig. 3(b) we observe a bimodal distribution. For Titania, $v_0 = 0.033\,\mathrm{nm}^3$ and $a_0 = 0.499\,\mathrm{nm}^2$. The incepted particles from the gas-phase dominate the PSD at very early times (10 ms) and the secondary peak is barely visible, however at slightly later times (100 ms) the secondary peak becomes more noticeable. At much later times (Fig. 3(c) and Fig. 3(d)) the distribution has become unimodal as coagulation becomes the predominant mechanism in the system.

Figure 4 shows how the system is affected at lower temperatures. We see from Fig. 4(a) that the average diameter of TiO_2 particles is reduced as the temperature falls. This effect is caused in part by the reduction in the rate of coagulation (proportional to $T^{1/2}$) but mainly by the reduction in the concentration of particles in the system (Fig. 4(b)) caused by the reduction in the rate of particle inception.

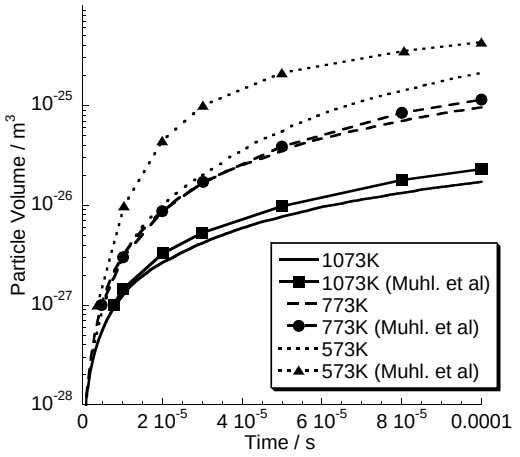

(a) Average volume of particles against time

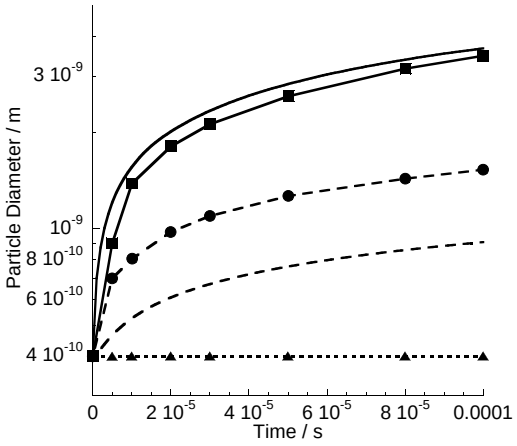

(b) Average diameter of particles against time

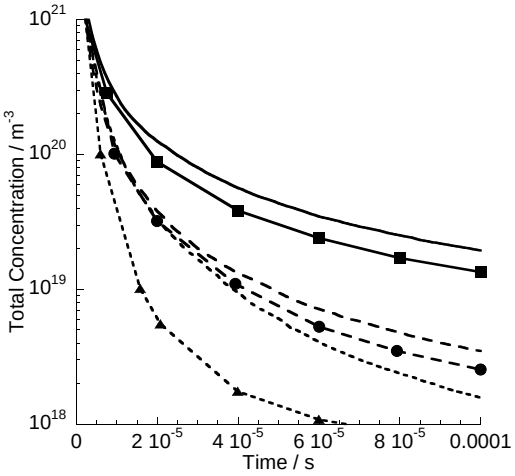

(c) Total concentration of particles against time

Figure 1: Comparison of various SiO_2 particle properties at various temperatures.

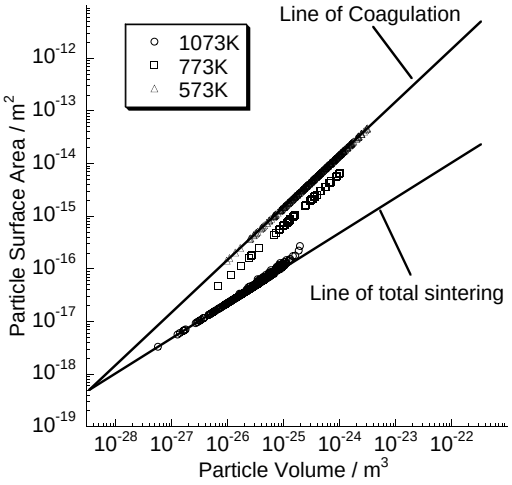

Figure 2: Average surface area against the average volume of particles at various temperatures.

Table 2: *Parameters for* TiO_2 *system.*

Parameter	Value
$C_0(TiCl_4)$	$5 \times 10^{-6}\,\mathrm{mol\,m^{-3}}$
t_{stop}	$10.0\,\mathrm{s}$
T	$800/1100/1400\,\mathrm{K}$
A(gas)	$8.26 \times 10^4\,\mathrm{s^{-1}}$
E_A/R(gas)	$10681\,\mathrm{K}$
A(surf.)	$49.0\,\mathrm{m\,s^{-1}}$
E_A/R(surf.)	$8993\,\mathrm{K}$
A_{sint}	$7.4 \times 10^8\,\mathrm{K^{-1}m^{-4}s}$
B_{sint}	$3.1 \times 10^4\,\mathrm{K}$

In Fig. 5 we investigate the effect of increasing the initial concentration of the precursor ($TiCl_4$), with both particle inception and surface growth simulated (denoted 'SG') and with particle inception only (denoted 'no SG'). Figure 5(a) and Fig. 5(b) show that at high concentrations, surface oxidation causes the marginal PSDs for both volume and area to be shifted to the right. At lower concentrations, the PSDs remain the same irrespective of surface growth. The figures support the conclusion reached in [8] that surface oxidation is more relevant at high concentrations of $TiCl_4$. In contrast however to one of the conclusions reached in [9] we see that surface oxidation causes a noticeable effect even when taking the total oxidation rate of $TiCl_4$ to be $k_{\mathrm{tot}} = k_{\mathrm{g}} + k_{\mathrm{s}} A_s$ as opposed to the model mentioned in [9].

5 Conclusion

We investigated a model that includes four mechanisms for nanoparticle evolution: coagulation, particle inception, surface growth and sintering. To simulate this model, we used a mass-flow stochastic particle system to generate the evolution of the PSDF without the great computational expense of other numerical techniques. The stochastic particle method was able to illustrate the many subtleties associated with the model; sintering is affected by temperature and particle size, when particle inception is included a bimodal distribution is initially established, and that surface growth is dependent upon high precursor concentrations.

The simplicity of the stochastic algorithm and its high computational efficiency should allow simulations to be coupled to computational fluid dynamics simulations so that particle-flame models may be solved without having to resort to simple, monodisperse models that cannot elucidate the subtleties of the particle size distributions.

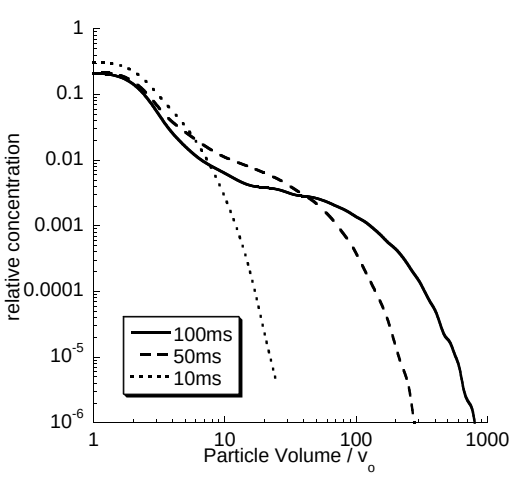

(a) PSD of particle volumes at early times

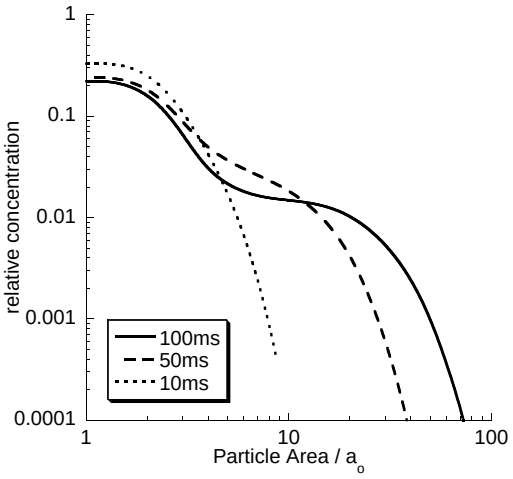

(b) PSD of particle areas at early times

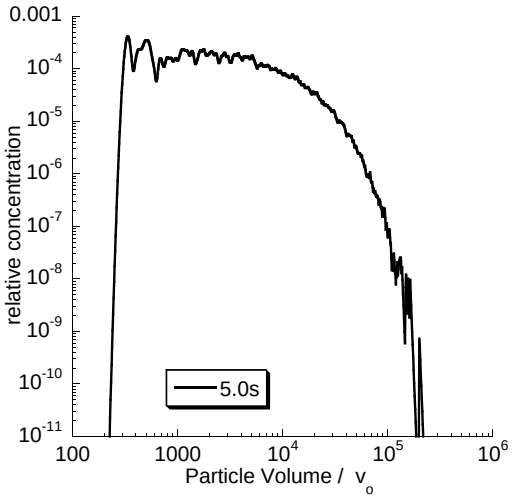

(c) PSD of particle volumes at late times

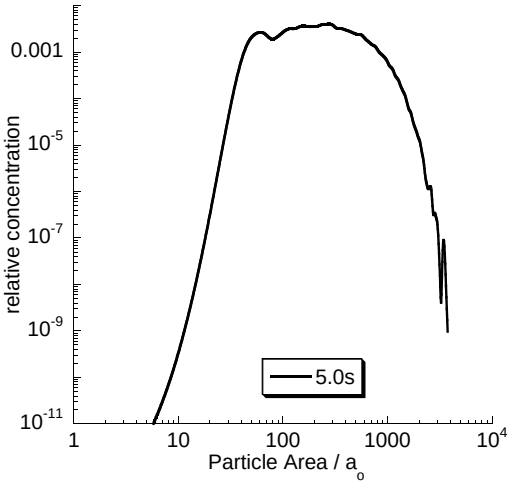

(d) PSD of particle areas at late times

Figure 3: PSDs of TiO_2 particle system at various times ($T = 1400\,\mathrm{K}$).

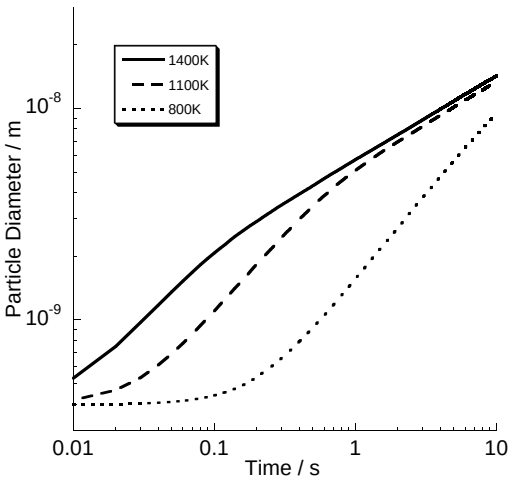

(a) Average diameter of TiO_2 particles

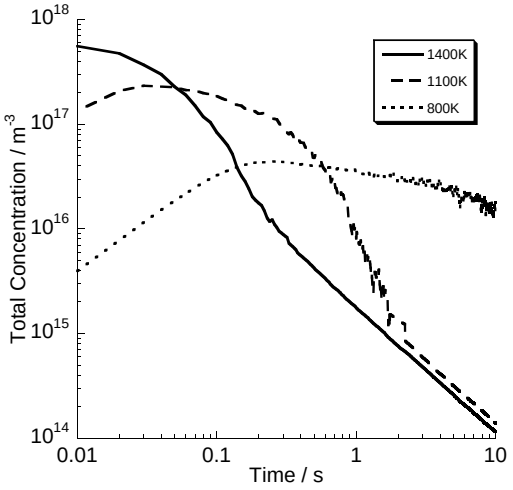

(b) Concentration of TiO_2 particles

Figure 4: Various particle properties at varying temperatures.

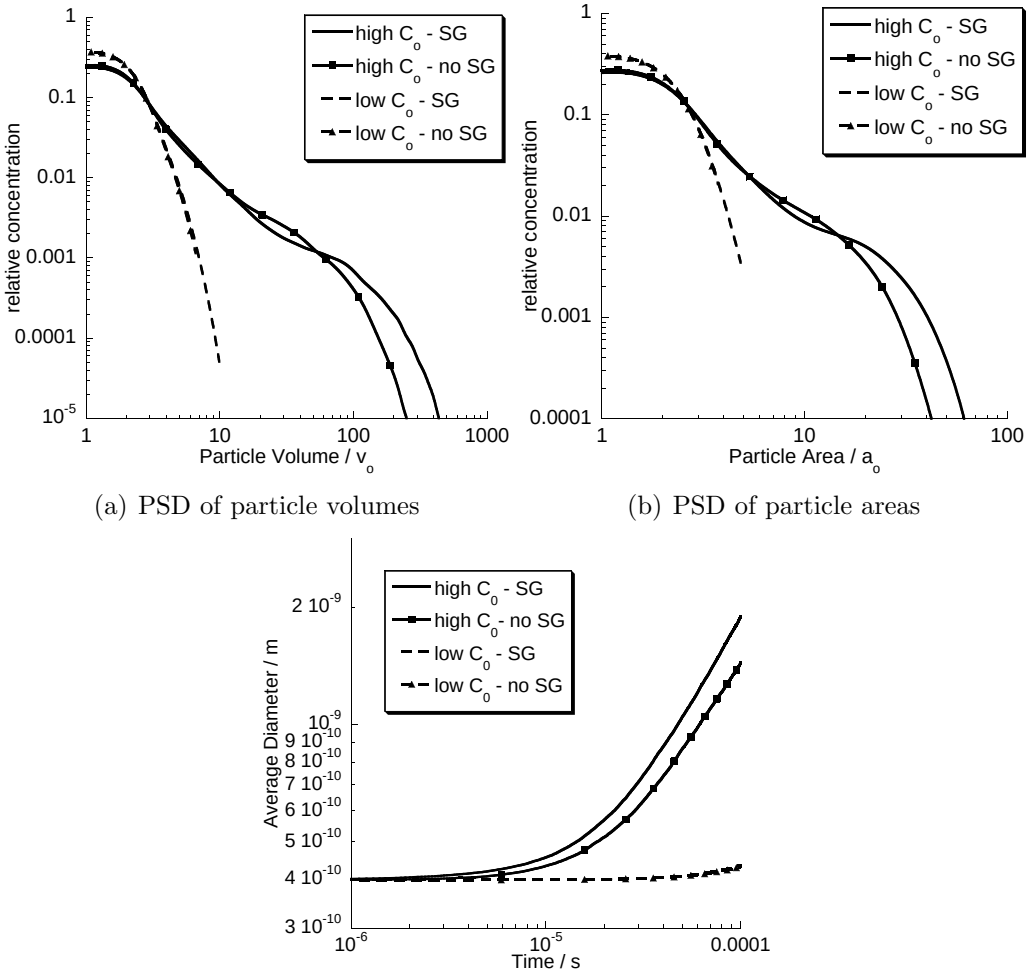

(a) PSD of particle volumes

(b) PSD of particle areas

(c) Average diameter of TiO_2 particles

Figure 5: PSDs and average diameter of TiO_2 particles when simulated with and without surface growth at high initial concentration of $TiCl_4$. For high initial concentration, $1.0\,\mathrm{mol\,m^{-3}}$, whilst for low initial concentration, $0.01\,\mathrm{mol\,m^{-3}}$.

6 Acknowledgements

The authors would like to thank the EPSRC (grant number GR/R85662/01) for the financial support of Neal Morgan under the title 'Mathematical and Numerical Analysis of Coagulation-Diffusion Processes in Chemical Engineering' and the Oppenheimer Fund for the support of Clive Wells.

References

[1] Andreas Eibeck and Wolfgang Wagner. Stochastic particle approximations for smoluchowski's coagulation equation. *SIAM J. Sci. Comput.*, 22(3):802–821, 2000.

[2] M. Goodson and M. Kraft. An efficient algorithm for simulating nano-particle dynamics. *Journal of Computational Physics*, 183:210–232, 2002.

[3] D. Grosschmidt, H. Bockhorn, M. Goodson, and M. Kraft. Two approaches to the simulation of silica particle systems. *Proc. Combust. Inst.*, 29:1039–1046, 2002.

[4] F.E. Kruis, K.A. Kusters, B. Scarlett, and S.E. Pratsinis. A simple model for the evolution of the characteristics of aggregate particles undergoing coagulation and sintering. *Aerosol Science and Technology*, 19:514, 1993.

[5] D. Lindackers, M.G.D. Strecker, P. Roth, C. Janzen, and S. E. Pratsinis. Formation and growth of sio2 particles in low pressure h2/o2/ar flames doped with sih4. *Combustion Science and Technology*, 123:287–315, 1997.

[6] N.M. Morgan, C.G. Wells, M. Goodson, M. Kraft, and W. Wagner. Numerical modelling of nano-particles in premixed laminar flames. Technical Report 16 (to be submitted), c4e Preprint-Series, Cambridge, 2003.

[7] H. Mühlenweg, A. Gutsch, A. Schild, and S.E. Pratsinis. Process simulation of gas-to-particle-synthesis vis population balances: Investigation of three models. *Chemical Engineering Science*, 57:2305–2322, 2002.

[8] S.E. Pratsinis, H. Bai, P. Biswas, M. Frenklach, and S.V.R. Mastrangelo. Kinetics of $ticl_4$ oxidation. *Journal of the American Ceramics Society*, 73:2158–2162, 1990.

[9] S.E. Pratsinis and P.T. Spicer. Competition between gas phase and durface oxidation of ticl4 during synthesis of tio2 particles. *Chemical Engineering Science*, 53:1861–1868, 1998.

[10] D.E. Rosner and J.J. Pyykonen. Bivariate moment simulation of coagulating and sintering nanoparticles in flames. *Particle Technology and Fluidization*, 48(3):476–491, 2002.

[11] P.T. Spicer, O. Chaoul, S. Tsantilis, and S.E. Pratsinis. Titania formation by ticl4 gas phase oxidation, surface growth and coagulation. *Journal of Aerosol Science*, 33:17–34, 2002.

[12] Z. Sun, R.L. Axelbaum, and B.H. Chao. A multicomponent sectional model applied to flame synthesis of nanoparticles. *Proc. Combust. Inst.*, 29:1063–1069, 2002.

[13] P. Tandon and D.E. Rosner. Monte carlo simulation of particle aggregation and simultaneous restructuring. *Journal of Colloid and Interface Science*, 213:273–286, 1999.

[14] M. von Smoluchowski. Drei vortrge über diffusion, brownsche molekularbewegung und koagulation von kolloidteilchen. *Phys. Z.*, 17:557–571 and 585–599, 1916.

[15] C.G. Wells and M. Kraft. Direct simulation and mass flow stochastic algorithms to solve a sintering-coagulation equation. Technical Report 10, c4e Preprint-Series, Cambridge, 2003.

[16] Y. Xiong and S.E. Pratsinis. Formation of agglomerate particles by coagulation and sintering - part i. a two-dimensional solution of the population balance equation. *Journal of Aerosol Science*, 24(3):283–300, 1992.